Super-Resolution CEUS Imaging

Technical White Paper

Ouyang Yali, Sang Maodong, Zheng Zhilan
Ultrasound Imaging System Development Department, Mindray

Super-Resolution CEUS Imaging

1. Background

Blockage, obstruction and lesions of microcirculation are the precursors of many diseases. Microcirculation refers to the blood circulation between arterioles and venules in the vascular network. It is not only a peripheral part of the circulatory system, but also an important component of the organs. Under normal circumstances, the blood flow of microcirculation is adapted to the metabolic level of human tissues and organs, so as to maintain the normal life activities and metabolism of the human body. When the metabolism and function of tissues and organs are abnormal, microcirculation will change to a certain extent. Abnormal changes in microvessels are related to a variety of diseases, such as arteriosclerosis, diabetes, chronic kidney disease, liver fibrosis and cirrhosis, inflammatory bowel disease, and cancer[1][2][3]. For example, an important hallmark of cancer is the formation of pathological microvessels, which locally stimulate the growth of microvessels through the release of pro-angiogenic factors, thus providing nutrients for the growing malignant tumors[4]. In addition, compared with normal microvascular structures, pathological microvessels lack an orderly hierarchical structure, are branched and distributed unevenly, and have twisted and irregular blood vessels[2]. Therefore, early detection and characterization of pathological changes in microvessels has important clinical value for disease prevention, intervention, and treatment.

Doppler ultrasound imaging, as one of the widely used blood flow imaging methods, uses moving red blood cells as scatterers to improve the sensitivity of blood flow detection. However, it is difficult for traditional Doppler ultrasound to detect small vessels with relatively slow blood flow (<1 cm/s) due to the limited presence of weak scatterers in small vessels and their slower moving velocity[5]. Ultra-sensitive Doppler imaging uses ultra-high-velocity plane wave imaging and spatio-temporal filtering methods to greatly improve the sensitivity of traditional Doppler ultrasound and improve the detection ability of small blood vessels. However, it still cannot reach the microscopic scale and is difficult to effectively display arterioles and venules[5][6][7]. In order to enhance blood flow imaging, contrast-enhanced ultrasound (CEUS) imaging technology is used to enhance the contrast of blood flow echo signals by injecting contrast agents. It is a necessary examination method for clinical evaluation of blood flow circulation and perfusion. However, the theoretical spatial resolution of CEUS and conventional ultrasound imaging is limited by the diffraction limit of ultrasound[8] (approximately equal to the ultrasound wavelength. For example, for the ultrasound waves propagating in the human body with frequencies from 15 MHz to 1.5 MHz, the wavelength range is approximately 100 μm to 1000 μm).

In recent years, the introduction of Ultrasound Localization Microscopy (ULM) technology has greatly improved the spatial resolution of ultrasound in microvascular imaging [9][10][11]. Inspired by optical fluorescence positioning microscopy, ULM detects and separates microbubble signals in a continuous image sequence, then accurately positions each microbubble and tracks the microbubble movement trajectory, and finally reconstructs blood vessel images with a resolution of micron level. The ULM technology breaks through the diffraction limit of traditional ultrasound imaging, also known as Super-Resolution imaging.

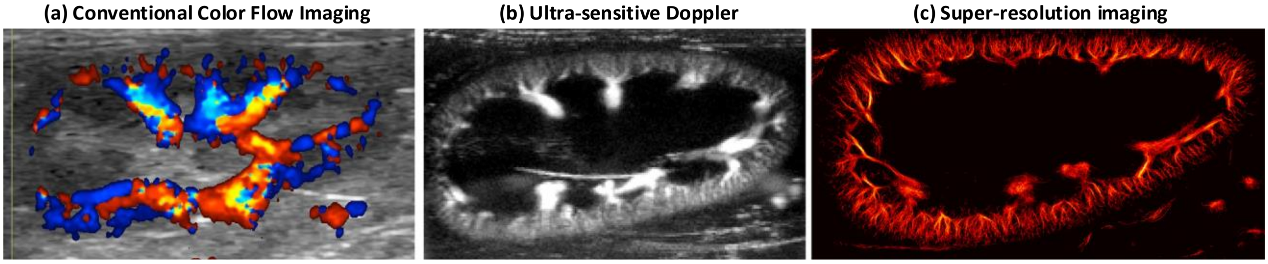

Figure 1 Ultrasound blood flow image of rabbit kidney: (a) Conventional Color Flow imaging; (b) Ultra-sensitive Doppler imaging; (c) Super-Resolution imaging[12]

Compared with traditional ultrasound imaging, ULM improves the spatial resolution of images by nearly 10 times[5][10][13]. However, as an emerging technology, ULM imaging still faces some challenges from laboratory to clinical application. Although researchers have used conventional clinical ultrasound equipment to conduct human ULM imaging research[14][15][16], the temporal resolution of data collected at low frame rates (ten to tens of Hz) is low, making it difficult to accurately position and track fast-moving microbubbles, which has a certain impact on the imaging performance of ULM[17]. Therefore, researchers usually need to dilute the microbubbles so that the algorithm can accurately position spatially separable microbubbles. However, in actual applications, due to various factors such as different patients, organs, applications, and contrast agent concentrations between different manufacturers, in order to maintain a certain level of microbubbles in the blood flow, diluted microbubbles may need multiple injections or slow continuous injection[16][18], which increases the difficulty of the doctor's operation.

In addition, in order for ULM imaging to fully present blood flow information, enough microbubbles are required for accumulation. Therefore, the combination of microbubble dilution and low frame rate will inevitably increase the data collection time. As mentioned in the literature, it is necessary to continuously collect data on the same imaging plane for tens of seconds or even minutes[19][20]. This is very challenging for doctors to stably hold the probe to scan on the same imaging plane, especially for applications in abdominal organ imaging that is also easily affected by respiratory motion. The displacement caused by respiratory motion is significantly larger than the diameter of the microvessels, making motion correction difficult. Although the effects of respiratory motion can be reduced by holding the patient's breath, the breath-holding time is limited and is not suitable for long-term data collection. In addition, existing research is mostly based on superficial ULM imaging in small-sized animals or humans, which is difficult to meet the requirements of clinical application scenarios deep in the human body (for example, abdomen and transcranial)[10][14][18]. Demené et al. used the phased array ultrasound imaging with ultra-fast frame rate to achieve ULM imaging depth of more than 10 cm in adult cranial blood vessels for the first time, but the microbubbles needed to be diluted and the data collection time was more than 2 minutes[21]. In addition, the amount of data processing and calculation for ULM reconstruction of each frame of image is very large and time-consuming. Therefore, all studies rely on offline post-processing. That is, the data collection equipment and processing equipment are separated. This inconvenience also restricts the clinical application of the technology. Applications are currently mainly focused on preclinical research on small-sized animals or superficial lesions of human[5][10][14][18][22].

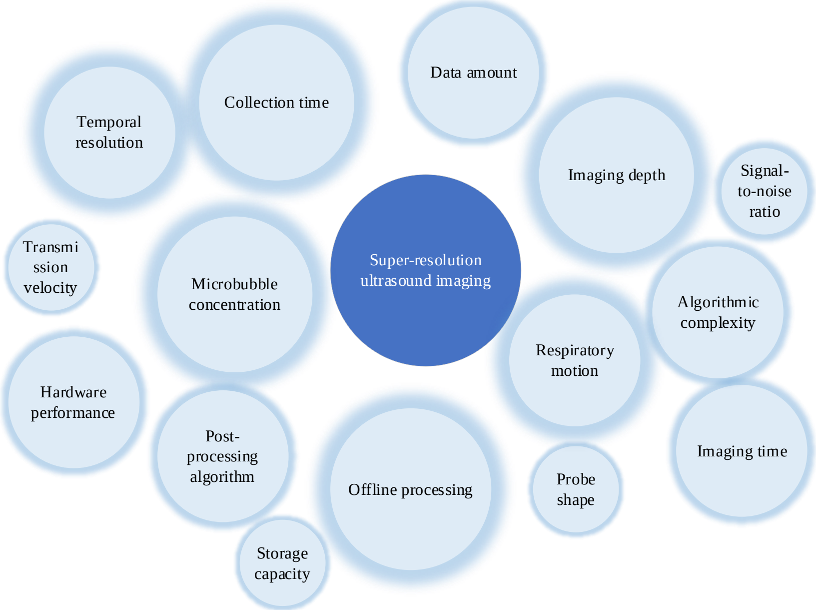

Figure 2 Restrictions on the clinical application of Super-Resolution ultrasound imaging

2. Super Resolution CEUS Imaging Overview

The Super-Resolution CEUS imaging (SR CEUS) function installed on the Mindray Resona A20 ultrasound imaging platform can collect data within 10 seconds under the condition of injecting a conventional concentration dose of contrast agents, and complete the calculation and display of Super-Resolution images on the machine. In the collection time of only a few seconds, the patient can control the breath hold and the clinician can easily keep the probe stable while holding it. It is stable and can effectively reduce the impact of breathing or probe motion on imaging reconstruction in the imaging plane. It is the first time that Super-Resolution imaging can detect microcirculatory changes in the early stages of diseases in a clinical environment.

In terms of data collection, by leveraging the industry-leading beamforming computing and powerful GPU/CPU processing, the Resona A20 imaging platform uses linear array plane wave/convex array divergent wave imaging technology to achieve ultra-high frame rate imaging (about 500 frames/s) of different probe types. The front-end beamformed in-phase/quadrature IQ data collected by Super-Resolution imaging can provide more time-frequency information than the movie data collected by traditional low frame rate equipment. In terms of algorithm processing, efficient spatiotemporal filtering, motion compensation, microbubble positioning and tracking algorithms are designed to perform a series of Super-Resolution imaging processing on the collected IQ data, and can generate four kinds of imaging results of microvessel morphology and hemodynamics (vessel density imaging, flow velocity imaging, flow direction imaging, and Bi-directional vessel density imaging) within 1-2 minutes. In terms of quantitative analysis, in order to further improve the clinical application value of Super-Resolution CEUS imaging, three quantitative analysis parameters (vessel diameter and spacing, vessel density, and vessel density ratio) are also provided to assist doctors in further analyzing and diagnosing lesions from microscale images.

2.1 Data Collection

Traditional ultrasound imaging adopts the focused linear scan mode. Each emission can only image a small area. Each imaging line obtained requires at least one focusing of the transmitting beam and the focusing of the receiving beam. The imaging frame rate is limited, as shown in Figure 3(a). Depending on the actual application and imaging depth, traditional focused imaging methods can only achieve imaging frame rates ranging from a few hertz to tens of hertz. Traditional focused imaging methods have low temporal resolution and are difficult to accurately position and track fast-moving microbubbles[21]. In addition, the imaging results obtained by the traditional linear scan method are not time-synchronous. There is a large time interval between columns in the collected imaging frames. This will cause the spatio-temporal correlation of the echo signal to weaken, which is not conducive to the extraction of microbubble signals and the filtering of tissue and noise signals.

In order to more stably and continuously capture the movement trajectory of each microbubble, Super-Resolution CEUS imaging adopts ultra-high frame rates for data collection. The Resona A20 linear array and convex array probes use plane wave and divergent wave imaging technologies respectively to achieve ultra-high frame rate imaging. Based on non-focused emission technology (shown in Figure 3(b)) and using ultra-wide beam multi-angle emission, the spatial information of the entire area of interest can be obtained in one emission without the need for multiple emission. Compared with traditional linear scanning, the imaging frame rate is increased by hundreds of times, enabling ultra-fast ultrasound imaging. In addition, in order to improve image penetration and spatial resolution, ultra-wide beam processing is combined with multi-angle coherent recombination, and the combined imaging frame rate reaches 500 frames/s, as shown in Figure 4.

Super-Resolution CEUS imaging is based on microbubble positioning and tracking accumulation, and is very sensitive to inter-frame motion. Long-term data collection will inevitably introduce more motion interference (such as respiratory motion, stability of the hand-held probe, etc.). Based on the ultra-fast ultrasound imaging method, data is collected for a few seconds during the user's breath-holding period, which not only effectively reduces the data collection time, but also effectively reduces the impact of motion. Compared with traditional data collection at low frame rate, ultra-high frame rate imaging can quickly detect the instantaneous flow state of microbubbles. A large number of temporally adjacent images provide richer spatio-temporal information, which is conducive to the detection, precise positioning and tracking of microbubbles[23].

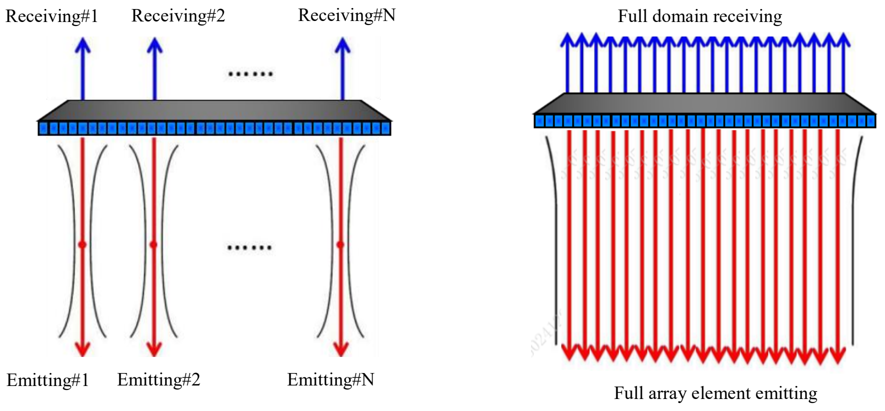

(a) Traditional focused emission (b) Unfocused emission

Figure 3 Schematic diagram of traditional focused emission and unfocused emission

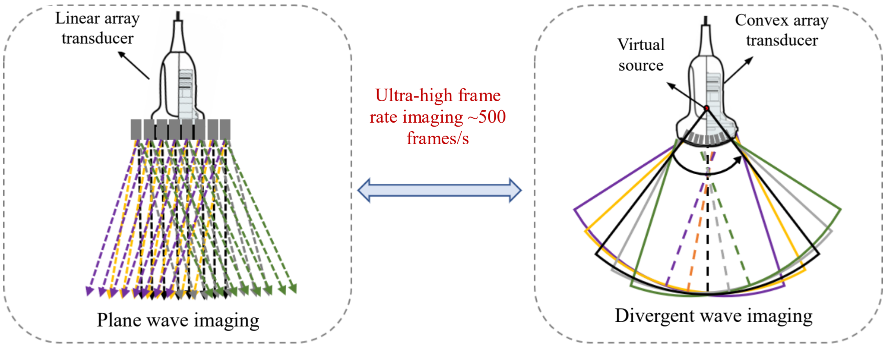

Figure 4 Multi-angle deflection emissions of linear array plane wave and convex array divergent wave

2.2 Imaging Processing

Figure 5 shows the Super-Resolution CEUS imaging data processing flow. After collecting echo signal data containing microbubbles for several seconds, the microbubble signals are extracted through signal detection and tissue suppression processing, and then all isolated microbubbles in each frame of data are identified and positioned and their displacements are tracked with sub-wavelength resolution. Each positioning point represents a microbubble, and microvessel morphology imaging can be generated through the accumulation of microbubble points. The inter-frame displacement of microbubbles represents the velocity of microbubble motion. After obtaining the precise positioning of each microbubble, the motion trajectory of the microbubbles is continuously tracked through multiple frames of data, and the velocity and direction of the microbubbles are estimated based on the motion trajectory of the microbubbles, thereby generating microhemodynamic imaging.

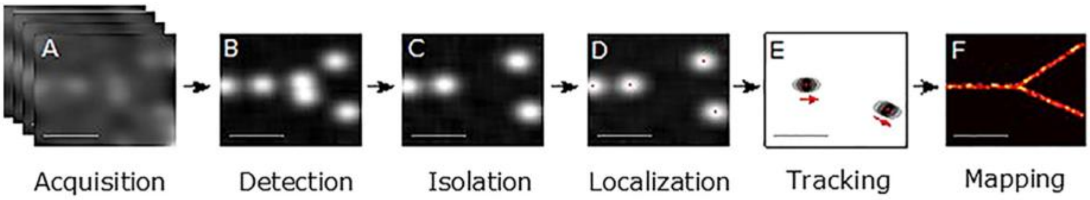

Figure 5 Super-Resolution imaging data processing flow[5]

2.2.1 Microbubble Detection and Extraction

Microbubble detection and extraction refers to the method of distinguishing the echo components of microbubbles from tissue and noise through signal processing, and using them for subsequent imaging processing. The processing quality of this link will directly affect the difficulty of subsequent microbubble positioning and the signal-to-noise ratio of the Super-Resolution CEUS imaging results. Insufficient detection of microbubbles means longer data collection time is required to obtain sufficient positioning results for final imaging.

Super-Resolution CEUS imaging makes full use of rich raw data containing microbubble information obtained by means of ultra-fast ultrasound imaging, combines the two-dimensional spatial and temporal information of the signals, and distinguishes the tissue and blood flow signals through their different spatio-temporal characteristics. In the raw data collected, there are three main signal components, namely, tissue signal, microbubble signal and noise. As shown in Figure 6, according to the spatio-temporal filtering theory, the eigenvalues represented by signal energy correspond to the signal components. Among them, the tissue echo signal has the strongest energy, concentrated in the first few larger eigenvalues. The flowing microbubble signal takes the second place, concentrated in subsequent eigenvalues. The noise signal has the weakest energy, corresponding to smaller eigenvalues[24]. Eigenvalues and eigenvectors correspond to each other and different signal components can be reconstructed. Therefore, the detection and extraction of microbubble signals can be implemented by using the spatio-temporal filtering method to filter the ultrasound imaging sequence.

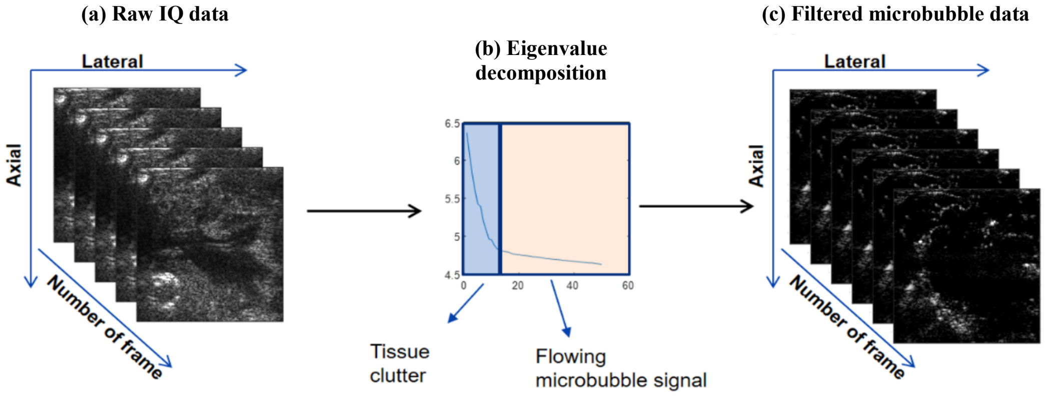

Figure 6 Schematic diagram of spatio-temporal filtering processing

2.2.2 Microbubble Positioning and Tracking

Generally, the diameter of contrast agent microbubbles is 2-10 μm. However, due to the limitation of diffraction effect in traditional ultrasound imaging, microbubbles will appear as larger "round spots" after being excited by ultrasound. The result of superposition of several frames of data is a larger "cloud group", and information such as the location and number of microbubbles cannot be distinguished. In contrast, Super-Resolution CEUS imaging locates the "centroid" of microbubbles in each frame of the image, in which the round-shaped microbubbles are replaced by small dots located at their centers of gravity. Based on the microbubble positioning information, the position and quantity of each microbubble can still be clearly observed in the result of superposition of several frames. Compared with traditional ultrasound imaging, the resolution will be greatly improved, and micron-level blood vessel imaging can be presentation.

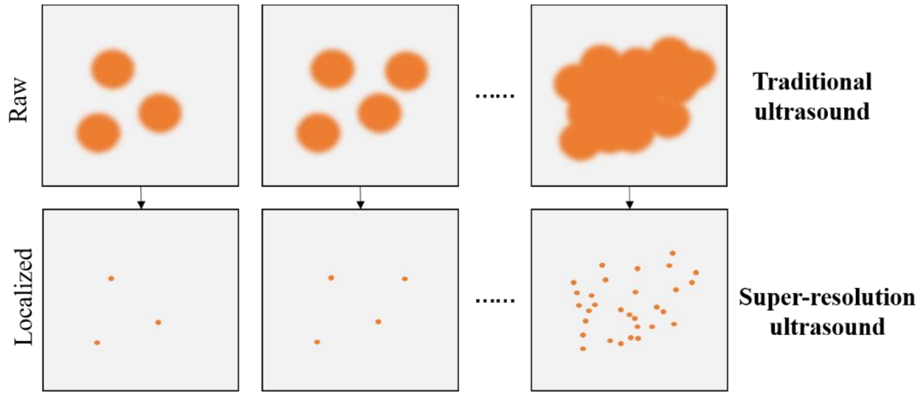

Figure 7 Schematic diagram of traditional ultrasound imaging and Super-Resolution ultrasound imaging

Another feature of Super-Resolution CEUS ultrasound is that it can image the velocity and direction of blood flow in small blood vessels. Microbubbles can move stably on multiple adjacent frames, resulting in a continuous microbubble motion trajectory in a 3D spatiotemporal matrix, as shown in Figure 8(a). On the contrary, random noise does not show any trajectory-like characteristics across multiple collected frames. Therefore, the characteristic differences between microbubbles and noise can be exploited in the spatio-temporal domain for noise suppression. Each microbubble trajectory in the 3D spatiotemporal matrix represents the spatial motion position of the microbubble over time, as shown in Figure 8(b). The direction and length of the microbubble trajectory can be determined by the motion velocity and direction of the microbubble. By calculating the direction and length of the microbubble trajectory, the flow velocity of the microbubbles can be obtained. This feature differs from that of traditional Doppler ultrasound, which uses the Doppler shift caused by the motion of red blood cells to measure blood flow velocity. Therefore, Super-Resolution CEUS ultrasound is not affected by common sources of errors in Doppler ultrasound (such as Doppler angle and spectral broadening) [12].

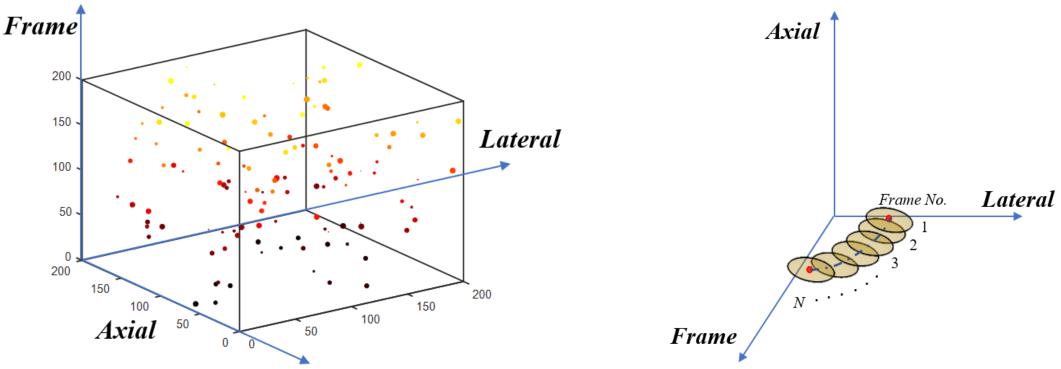

(a) Distribution of microbubbles in a 3D spatiotemporal matrix (b) Motion trajectory of a single microbubble in a 3D spatiotemporal matrix

Figure 8 Schematic diagram of microbubble positioning and tracking

As shown in Figure 9, by positioning each microbubble and tracking its displacement with sub-wavelength resolution, microvessel morphology images can be generated on the micron scale, and blood flow velocity and direction can be calculated to obtain microhemodynamic imaging.

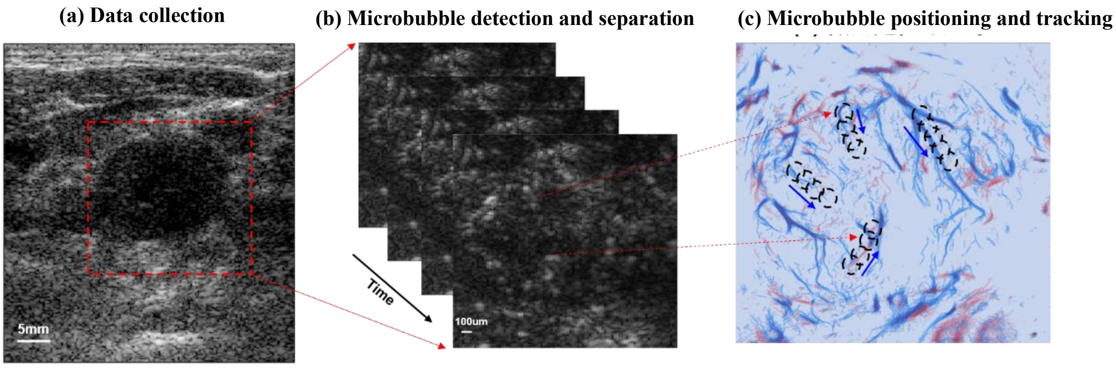

Figure 9 Super-Resolution CEUS ultrasound imaging workflow

2.3 Imaging Display

Super-Resolution CEUS imaging provides four different blood flow display methods, as shown in Figure 10. The display modes can be switched freely:

- Vas Density: The brighter the color scale bar, the higher the density of microbubbles; the darker the color scale bar, the lower the density of microbubbles.
- Flow Velocity: Different values of the color scale bar represent different blood flow velocities, the unit is mm/s.
- Flow Direction: The positive value of the color scale bar indicates a direction toward the probe, and the negative value indicates a direction away from the probe. The direction range is [-180°, 180°].
- VD Direction: The positive value of the color scale bar indicates a direction toward the probe, and the negative value indicates a direction away from the probe. The brighter the color scale bar, the higher the density; the darker the color scale bar, the lower the density.

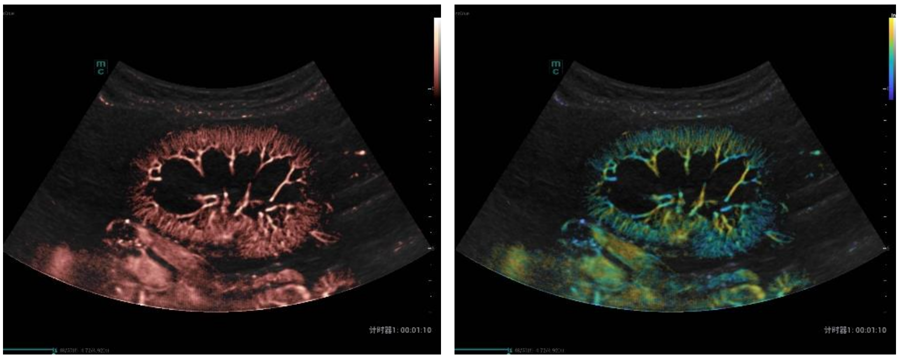

(a) Vas density imaging (b) Flow velocity imaging

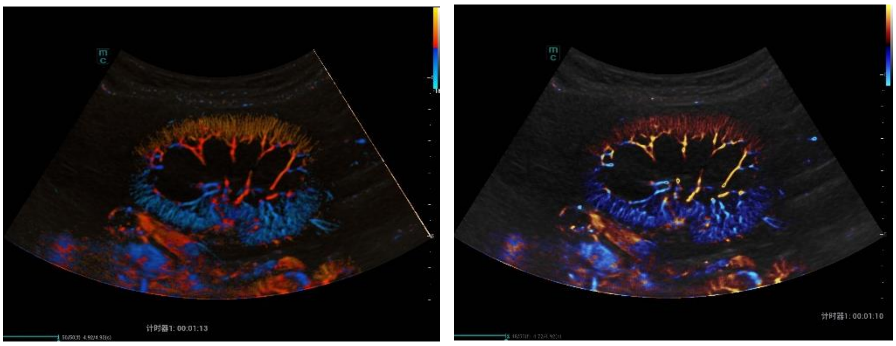

(c) Flow direction imaging (d) VD direction imaging

Figure 10 Super-Resolution CEUS imaging of canine kidneys

2.4 Quantitative Analysis

The occurrence, development or outcome of the disease is initially reflected at the microcirculation level. Normal microvessels are mainly composed of capillaries, arterioles, and venules, and have good fork-like branches and an orderly hierarchical structure. In contrast, tumor blood vessels lack an orderly hierarchical structure and are dilated, cystic, and uneven in diameter in terms of spatial distribution, as shown in Figure 11. Vessel density is related to tumor growth and metastasis, and is an important indicator to measure tumor angiogenesis. Some studies have shown that microvessel density is closely related to tumor grade, proliferation activity and other indicators[25]. Through quantitative analysis of parameters related to microvascular morphology and microhemodynamics, Super-Resolution CEUS imaging can be applied in the fields of identification of the nature of lesions, monitoring of progress, and quantitative evaluation of therapeutic effects.

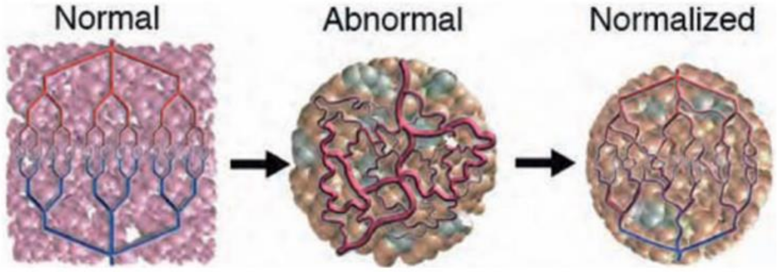

Figure 11 Evolution process of normal blood vessels, abnormal blood vessels, and blood vessels after treatment

(Science. 2005 Jan 7; 307(5706):58-62)

The Resona A20 platform provides quantitative analysis tools that match Super-Resolution CEUS imaging. Currently, quantitative analysis parameters include blood vessel distance (Distance), blood vessel density (VD), and blood vessel density ratio (VDR).

"Distance" is based on the microvessel density imaging results of Super-Resolution ultrasound and can be used to quantify the diameter of blood vessels and the distance between blood vessels. When the user draws a line of interest along the vertical direction of a blood vessel as much as possible on the microvessel density image, the system will automatically output the vessel profile curve at the corresponding position of the line of interest, automatically detect all blood vessels that the line of interest passes through, output the fitting curve corresponding to each blood vessel, as well as the maximum vessel diameter, minimum vessel diameter, and average diameter, and allow the user to further manually measure the distance between any vessels of interest. The diameter of blood vessels and the distance between blood vessels can reflect information about the local blood supply channels of tissues and can also evaluate the ability of Super-Resolution ultrasound imaging to detect changes in microvasculars in the early stages of the disease.

VD and VDR are important indicators for measuring tumor angiogenesis, as shown in Figure 12. Based on the microvessel density imaging results, VD is defined as the number of vessel pixels divided by the overall number of pixels of the tumor, and reflects the richness of blood flow. The tumor region can divide into peripheral and central regions according to the area. The VDR can be used to quantify the blood vessel distribution within the tumor central region and peripheral region, and can also be used to calculate the ratio of blood vessel density in the target area to the reference area. Based on the diversity of clinical scenarios, three VDR measurement methods are provided, namely, "VD Ratio-Fix" mode, "VD Ratio-Shell" mode, and "VD Ratio-Free" mode. In "VD Ratio-Fix" mode, the central region and peripheral region each account for 50% by default, which can be used to evaluate the tumor center and periphery/peripheral blood supply ratio. In "VD Ratio-Shell" mode, the thickness ratio of the central and peripheral regions is adjustable, which can be used for comparative evaluation of perfusion and morphology and expanded scenario applications (such as multi-modal). In "VD Ratio-Free" mode, different areas of interest can be freely drawn for comparative evaluation of the target area and the reference area.

$$\mathbf{VD\%} = \frac{\boldsymbol{Vessel\ pixels}}{\boldsymbol{overal\ tumorpixels}} \times 100 \qquad \mathbf{VDR} = \frac{\boldsymbol{Peripheral\ VD}}{\boldsymbol{center\ VD}}$$

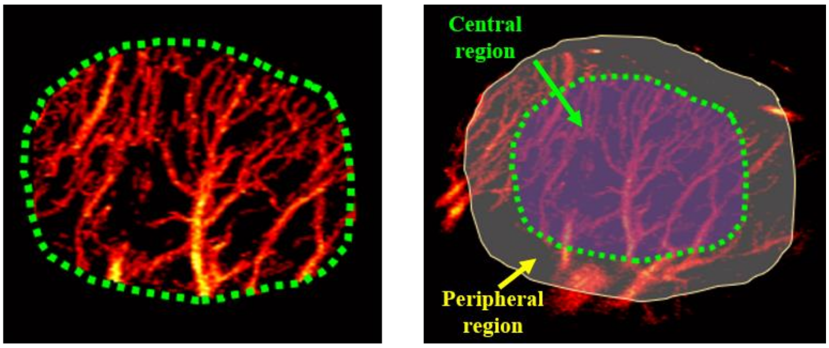

Figure 12 Calculation of VD and VDR based on Super-Resolution CEUS imaging (a) The green dotted line represents the tumor boundary. (b) The purple shaded area represents the tumor central region, and the gray shaded area represents the tumor peripheral region.

3. Super-Resolution CEUS Imaging Features

- **Conventional contrast agent concentration:** The contrast agent concentration is consistent with the current clinical routine contrast injection method and dosage. No concentration dilution is required.
- **Short collection time:** Under high frame rate (about 500 frames/s) collection conditions, not only can a large amount of time-continuous data be collected in a short time, but also motion interference can be effectively reduced through the patient's breath-holding control for several seconds.
- **Dynamic imaging:** Equipped with the Resona A20 high-efficiency system architecture and computing platform, the transmission, storage and computing efficiency of the Super-Resolution CEUS function are significantly improved (imaging calculation only takes 1-2 minutes), enabling on-machine dynamic imaging. (Imaging calculations in labs usually do not count time costs, which may cost even up to a day.)
- **High spatial resolution:** Super-Resolution CEUS technology breaks through the diffraction limit of traditional ultrasound imaging and can achieve higher spatial resolution, provides images of micro-vessels, and captures information on changes in microstructure in the early stages of disease.
- **Deep imaging penetration:** Super-Resolution CEUS technology not only has higher spatial resolution, but also obtains clear images within a larger imaging depth range, breaking through the restrictive relationship between depth and high-resolution imaging, which has great significance for observing microstructural changes in deep tissues.
- **Multi-parameter quantification:** Super-Resolution CEUS technology provides a variety quantization parameter. Based on quantitative analysis, specific and sensitive diagnostic indicators can be obtained, which has important clinical significance in assisting clinical diagnosis, prognosis, monitoring and treatment.

4. Super-Resolution CEUS Imaging Case Sharing

Case 1: Focal nodular hyperplasia of human liver

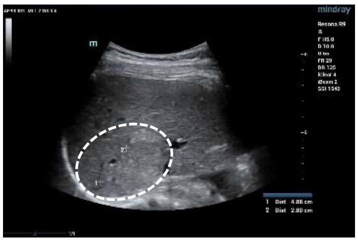		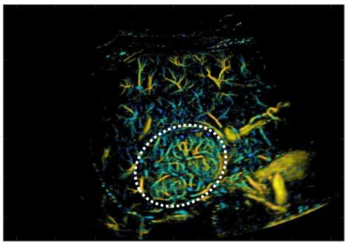
a. Grayscale imaging	b. Microvessel density imaging	c. Microvessel blood flow velocity imaging

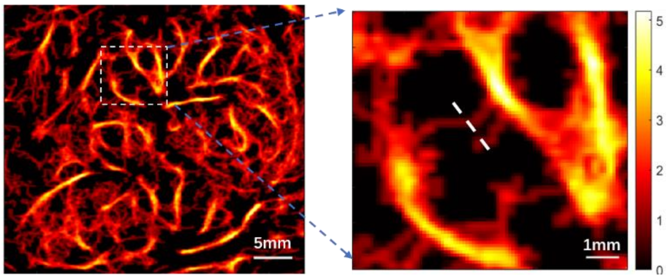	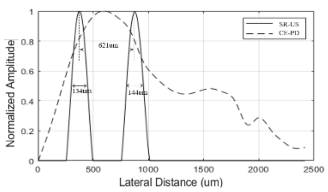
d. Sampling the line within the lesion	e. Inner diameters of two microvessels, which are 134 μm and 144 μm respectively

Case description: Super-Resolution CEUS enables **imaging of deep lesions** using an abdominal convex array probe. Compared with the sparse and orderly distribution of blood vessels in normal liver tissues, microvessel density imaging (b) of focal nodular hyperplasia (FNH) of the liver shows that microvessels are distributed in a "spoke-like" shape, and the vessel density is significantly increased compared with normal liver tissue. Microvessel blood flow velocity imaging (c) shows that the flow velocity gradually decreases from the center to the periphery. The distance measurement of microvessels within the lesion (d, e) shows that the inner diameters of two microvessels in the area of interest are 134 μm and 144 μm respectively. This technology not only breaks through the half-wavelength resolution limit, but also breaks through the relationship between ultrasound penetration and resolution.

Remarks: The depth of the nodule is 8.6 cm, and the size of the nodule is 4.99 cm ×2.8 cm.

Figure 2 Super-Resolution CEUS imaging of human kidneys

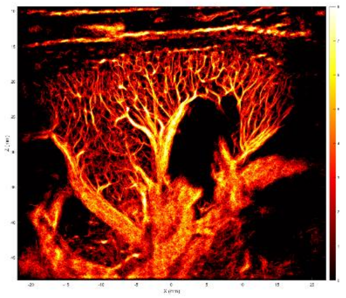	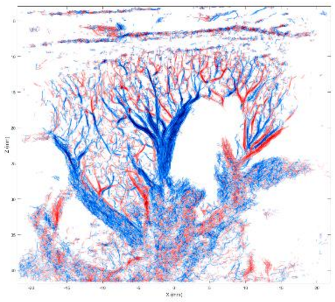	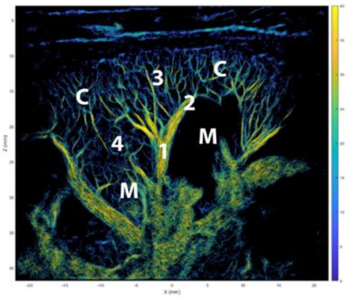
a. Microvessel density imaging	b. Microvessel Bi-directional vessel density imaging	c. Microvessel blood flow velocity imaging

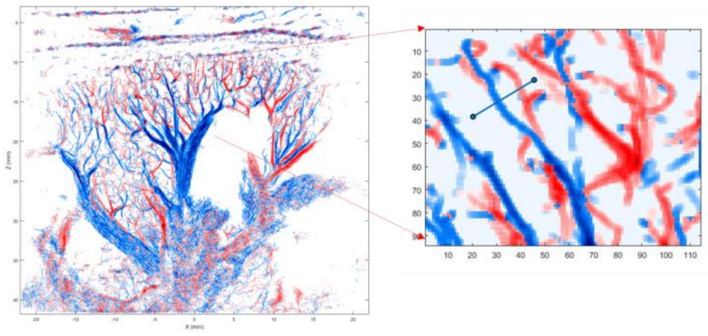	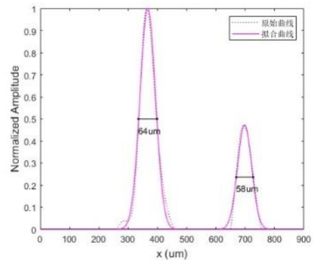
d. Measurement of the inner diameter of radial interlobular vessels in the cortex Blue: Interlobular veins Red: Interlobular arteries	e: Diameter of interlobular vein of 64 μm and diameter of interlobular artery of 58 μm

Case description: Super-Resolution CEUS imaging of human autologous kidney shows complete imaging of interlobular vessels-arcuate vessels-interlobular vessels, imaging of renal cortical radial interlobular vessels and part of the medullary recta blood vessels, and measurement of the inner diameter of interlobular vessels in the cortex. The diameters of interlobular veins and interlobular arteries are 64 μm and 58 μm. It breaks through the half-wavelength limit and achieves Super-Resolution imaging. It provides visual microstructural information for the evaluation of early microvascular changes in progressive renal disease or transplanted kidneys.

C: Renal cortex; M: Renal medulla; 1: Interlobular vessels; 2: Arcuate vessels; 3: Cortical radial interlobular vessels

4: Medullary recta blood vessels

Case 3: Canine craniocerebral imaging (peeling of the skull)

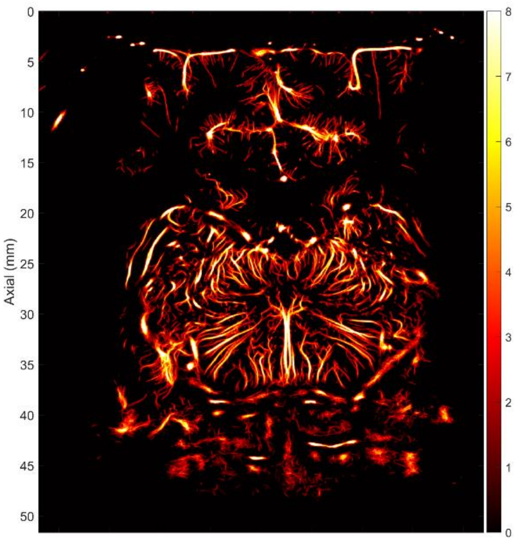

a. Microvessel density imaging

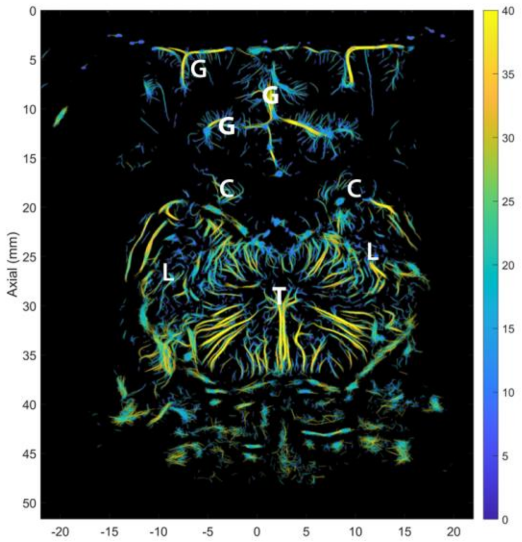

b. Microvessel blood flow velocity imaging

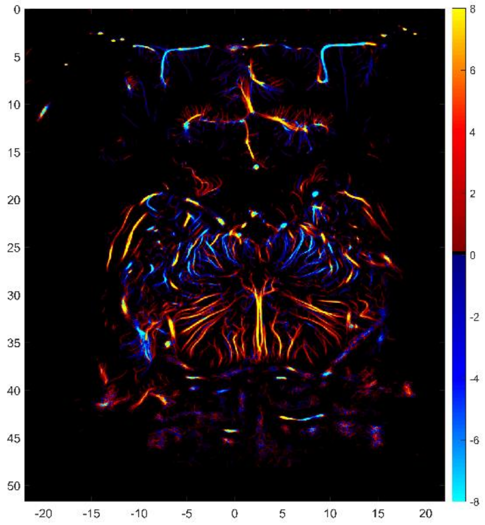

c. Microvessel Bi-directional vessel density imaging

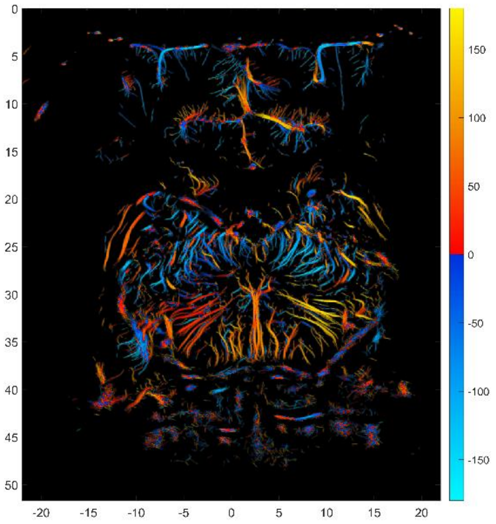

d. Microvessel blood flow velocity direction

Case description: Super-Resolution CEUS imaging of canine intracranial gyrus, thalamus, lentiform nucleus, caudate nucleus and other functional nuclei provides a visual basis for early identification of cerebral small-vessel disease. Cerebral small-vessel disease is a series of clinical, imaging, and pathological syndromes caused by various factors that affect small arteries and their distal branches, arterioles, capillaries, and venules in the brain. For example, subcortical small artery infarction can cause brain tissue hypoperfusion and brain parenchymal damage, leading to cognitive impairment, dementia and death risks.

G: Gyrus; C: Caudate nucleus; L: Lentiform nucleus; T: Thalamus

Note: The above three cases are summarized from offline simulation results. The clinical on-machine cases are subject to communication and authorization. The actual results are subject to the on-machine images.

5. Conclusion

Super Resolution CEUS technology used on the Mindray Resona A20 ultrasound imaging platform overcomes the limitations of traditional Super-Resolution imaging and pioneers the transformation of Super-Resolution imaging technology from pre-clinical research to clinical application. It has realized the clinical application of Super-Resolution imaging that meets the clinical environment and is equipped with the devices integrated with data collection, imaging, and analysis functions for the first time. Micron-level blood vessel morphology imaging and hemodynamic imaging break through the traditional ultrasound diffraction limit, make up for the shortcomings in penetration and resolution of existing biomedical ultrasound imaging, and achieve Super-Resolution microvessels at clinically relevant imaging depths. It provides a number of quantitative parameters for evaluating changes in microvascular structure and microcirculatory function in the early stages of the disease, which has important clinical significance in assisting clinical diagnosis, prognosis, monitoring and treatment.

6. References

[1] Cade W T. Diabetes-related microvascular and macrovascular diseases in the physical therapy setting[J]. Physical therapy, 2008, 88(11): 1322-1335.

[2] Goel S, Duda D G, Xu L, et al. Normalization of the vasculature for treatment of cancer and other diseases[J]. Physiological reviews, 2011, 91(3): 1071-1121.

[3] Ooi Q L, Tow F K N F H, Deva R, et al. The microvasculature in chronic kidney disease[J]. Clinical journal of the American Society of Nephrology: CJASN, 2011, 6(8): 1872.

[4] Hanahan D, Weinberg R A. Hallmarks of cancer: the next generation[J]. cell, 2011, 144(5): 646-674.

[5] Christensen-Jeffries K, Couture O, Dayton P A, et al. Super-Resolution ultrasound imaging[J]. Ultrasound in medicine & biology, 2020, 46(4): 865-891.

[6] Demené C, Deffieux T, Pernot M, et al. Spatiotemporal clutter filtering of ultrafast ultrasound data highly increases Doppler and fUltrasound sensitivity[J]. IEEE transactions on medical imaging, 2015, 34(11): 2271-2285.

[7] Baranger J, Arnal B, Perren F, et al. Adaptive spatiotemporal SVD clutter filtering for ultrafast Doppler imaging using similarity of spatial singular vectors[J]. IEEE transactions on medical imaging, 2018, 37(7): 1574-1586.

[8] Tang M X, Mulvana H, Gauthier T, et al. Quantitative contrast-enhanced ultrasound imaging: a review of sources of variability[J]. Interface focus, 2011, 1(4): 520-539.

[9] Couture O, Besson B, Montaldo G, et al. Microbubble ultrasound super-localization imaging (MUSLI)[C]//2011 IEEE International Ultrasonics Symposium. IEEE, 2011: 1285-1287.

[10] Errico C, Pierre J, Pezet S, et al. Ultrafast ultrasound localization microscopy for deep Super-Resolution vascular imaging[J]. Nature, 2015, 527(7579): 499-502.

[11] Christensen-Jeffries K, Browning R J, Tang M X, et al. In vivo acoustic Super-Resolution and super-resolved velocity maping using microbubbles[J]. IEEE transactions on medical imaging, 2014, 34(2): 433-440.

[12] Song P, Rubin J M, Lowerison M R. Super-Resolution ultrasound microvascular imaging: Is it ready for clinical use?[J]. Zeitschrift für Medizinische Physik, 2023.

[13] Couture O, Hingot V, Heiles B, et al. Ultrasound localization microscopy and Super-Resolution: A state of the art[J]. IEEE transactions on ultrasonics, ferroelectrics, and frequency control, 2018, 65(8): 1304-1320.

[14] Opacic T, Dencks S, Theek B, et al. Motion model ultrasound localization microscopy for preclinical and clinical multiparametric tumor characterization[J]. Nature communications, 2018, 9(1): 1-13.

[15] Dencks S, Piepenbrock M, Opacic T, et al. Clinical pilot application of Super-Resolution US imaging in breast cancer[J]. IEEE transactions on ultrasonics, ferroelectrics, and frequency control, 2018, 66(3): 517-526.

[16] Bodard S, Denis L, Hingot V, et al. Ultrasound localization microscopy of the human kidney allograft on a clinical ultrasound scanner[J]. Kidney International, 2023, 103(5): 930-935.

[17] Huang C, Zhang W, Gong P, et al. Super-Resolution ultrasound localization microscopy based on a high frame-rate clinical ultrasound scanner: An in-human feasibility study[J]. Physics in Medicine & Biology, 2021, 66(8): 08NT01.

[18] B. Liu, Y Yang, Q. He, J. Luo. Grading of Carotid Atherosclerotic Plaques using Super-Resolution Ultrasound Imaging: An in-vivo Feasibility Study. 2019 IEEE International Ultrasonics Symposium (IUS) Proceedings.

[19] Huang C, Lowerison M R, Trzasko J D, et al. Short acquisition time Super-Resolution ultrasound microvessel

imaging via microbubble separation[J]. Scientific reports, 2020, 10(1): 6007.

[20] Tang S, Song P, Trzasko J D, et al. Kalman filter-based microbubble tracking for robust Super-Resolution ultrasound microvessel imaging[J]. IEEE transactions on ultrasonics, ferroelectrics, and frequency control, 2020, 67(9): 1738-1751.

[21] Demené C, Robin J, Dizeux A, et al. Transcranial ultrafast ultrasound localization microscopy of brain vasculature in patients[J]. Nature biomedical engineering, 2021, 5(3): 219-228.

[22] Peng H, Qian X, Mao L, et al. Ultrafast ultrasound imaging in acoustic microbubble trap**[J]. Applied Physics Letters, 2019, 115(20).

[23] Gong P, Song P, Huang C, et al. Ultrasensitive ultrasound microvessel imaging for characterizing benign and malignant breast tumors[J]. Ultrasound in medicine & biology, 2019, 45(12): 3128-3136.

[24] Brown J, Christensen-Jeffries K, Harput S, et al. Investigation of microbubble detection methods for Super-Resolution imaging of microvasculature[J]. IEEE transactions on ultrasonics, ferroelectrics, and frequency control, 2019, 66(4): 676-691.

[25] Messiou C, Orton M, Ang J E, et al. Advanced solid tumors treated with cediranib: comparison of dynamic contrast-enhanced MR imaging and CT as markers of vascular activity[J]. Radiology, 2012, 265(2): 426-436.

mindray

healthcare within reach